European Radiology (2020) 30:4633–4640
https://doi.org/10.1007/s00330-020-06762-4

CONTRAST MEDIA

The anterior eye chamber: entry of the natural excretion pathway of gadolinium contrast agents?

Katerina Deike-Hofmann[1] · Paula von Lampe[2] · Heinz-Peter Schlemmer[1] · Nikolaos Bechrakis[3] · Christoph Kleinschnitz[4] · Michael Forsting[2] · Alexander Radbruch[2]

Received: 8 January 2020 / Revised: 13 February 2020 / Accepted: 19 February 2020 / Published online: 16 March 2020

Abstract

Objective Previous studies provided evidence that gadolinium can be found in the aqueous chamber (AC) of the eye several hours post injection (p.i.) of gadolinium-based contrast agents (GBCAs). This study aimed to investigate whether gadolinium can be detected promptly after injection of a macrocyclic GBCA on contrast-enhanced T1-weighted MRI in the AC of children.

Methods This retrospective study encompassed MRI of 200 healthy eyes of children suffering from retinoblastoma of the contralateral eye. MRI was performed with an orbital coil with the children in a state of general anesthesia. Differences of signal intensity ratios (ΔSIRs) of the AC to the lens were determined between pre and post contrast-enhanced T1-weighted images (Dotarem®, Guerbet, 0.1 ml/kg body weight, mean (standard deviation) p.i. time = 12:24 (± 2:31) min).

Results A highly significant signal intensity increase was found in the AC of healthy eyes 12 min after GBCA injection (median ΔSIR (interquartile range) = + 0.08 (0.05–0.12), $p < 0.0001$). In addition, gadolinium enhancement showed a strong negative correlation with children's age in multivariate analysis with adjustment for p.i. time ($p < 0.0001$).

Conclusions GBCA leakage into the AC of healthy infantile eyes was found promptly after injection. The negative correlation between patient age and GBCA enhancement might be explained by a maturation process of the blood-aqueous barrier or Schlemm's canal. Future studies should assess the duration and potential diagnostic applications as well as possible safety concerns of gadolinium presence in the AC.

Key Points

- *Leakage of gadolinium-based contrast agent into the aqueous chamber of infantile eyes was found promptly after intravenous injection ($p < 0.0001$).*
- *Gadolinium enhancement of the anterior eye chamber was negatively correlated with the children's age ($p < 0.0001$).*

Keywords Magnetic resonance imaging · Contrast media · Gadolinium · Anterior chamber · Eye

Electronic supplementary material The online version of this article (https://doi.org/10.1007/s00330-020-06762-4) contains supplementary material, which is available to authorized users.

✉ Katerina Deike-Hofmann
k.deike@dkfz.de

[1] Department of Radiology, German Cancer Research Center DKFZ, Im Neuenheimer Feld 223, 69120 Heidelberg, Germany

[2] Department of Radiology, University Clinic Essen, Essen, Germany

[3] Department of Ophthalmology, University Clinic Essen, Essen, Germany

[4] Department of Neurology, University Clinic Essen, Essen, Germany

Abbreviations

ΔSIR	Difference of anterior chamber-to-lens signal intensity ratio
AC	Aqueous chamber / anterior chamber
CNS	Central nervous system
CSF	Cerebrospinal fluid
FoV	Field of view
GBCA	Gadolinium-based contrast agent
GS	Glymphatic system
IQR	Interquartile range
MRI	Magnetic resonance imaging
p.i.	Post injection
ROI	Region of interest
SD	Standard deviation
SI	Signal intensity
SIR	Anter chamber-to-lens signal intensity ratio

Introduction

Recent studies showing long-term deposition of gadolinium-based contrast agents (GBCAs) within the brain have drawn attention to the excretion pathway of intravenously injected GBCAs [1–3]. Newly published studies provided evidence that GBCAs penetrate into the cerebrospinal fluid (CSF) and at least two concurrent pathways have been proposed as potential entry points: the choroid plexus and the aqueous chamber (AC) of the eye [2, 4].

To the best of our knowledge, no signal intensity (SI) increase on T1-weighted images in the AC following GBCA injection has been reported in healthy eyes so far and the scientific literature has paid little attention to a penetration of GBCAs into healthy eyes following intravenous GBCA injection. However, qualitative SI increase on fluid-attenuated inversion recovery MRI in the AC following ischemic brain injury has been termed abnormal and was reported to correlate positively with disease extent [5].

In our hospital, children suspicious of retinoblastoma are imaged in general anesthesia with pre and post contrast T1-weighting by using bilateral orbital coils to allow for exclusion of contralateral involvement. The orbital coils enable a superior resolution of the AC and might visualize excretion of the GBCA that cannot be detected on routine orbital MRI scans.

Therefore, the current retrospective study investigated pre and post contrast T1-weighted MRI of healthy, infantile eyes to test the hypothesis of the AC as an entry point for the GBCA into the central nervous system (CNS) following intravenous injection.

Patients and methods

Patients

This retrospective study was approved by the regional ethics committee. Written informed consent was waived due to the retrospective character of the study. Baseline MRI of 200 consecutive treatment naïve patients who were imaged at our institution between 2011 and 2019 due to the diagnosis of retinoblastoma was included in the study. Patients with bilateral retinoblastoma were excluded from the analysis.

MRI protocol

All patients were assessed at the same MRI scanner (1.5-T Siemens Aera) using a 4-cm loop coil. Identical T1-weighted images (repetition time 583 ms, echo time 16 ms, slice thickness 2.0 mm, flip angle 90°, voxel size 0.2 × 0.2 × 2.0 mm, field of view (FoV) read 80 mm, FoV phase 131.3%, 20 slices, distance factor 20%, acquisition time 7:53 min) were obtained prior and (mean ± standard deviation (SD)) 12:21 ± 2:36 min after injection of a single dose of gadoterate dimeglumine (Dotarem®, Guerbet, 0.1 ml/kg body weight). MRI was performed with the children in a state of general anesthesia induced by 1 ml propofol (1%) per kilogram of body weight.

For 25 healthy infantile eyes, T1-weighting was calculated with and without prescan normalization to assess its influence on AC-to-lens SI ratios (SIRs). SIRs with/without prescan normalization showed a strong linear correlation ($r_{Pearson} > 0.99$, $p < 0.0001$, Fig. 1e).

Image analysis

Image analysis was conducted on an accredited workstation by one of two readers after a prereading session with a neuroradiologist with 10 years of experience in radiology to warrant correct and reproducible SI measurements.

Regions of interests (ROIs) for SI measurements were drawn in the AC and the lens with the ROI encompassing the entire AC and lens on the slide with the largest diameter. Caution was drawn not to cross-anatomical boarders which might have resulted in inappropriate SI measurements (Fig. 1).

The SI ratio of the anterior chamber to the lens was calculated prior to and after GBCA injection and the difference (ΔSIR) was determined as follows:

$$\text{AC-to-lens } \Delta\text{SIR} = (\text{SI}(\text{AC}_{post})/\text{SI}(\text{lens}_{post})) - (\text{SI}(\text{AC}_{pre})/\text{SI}(\text{lens}_{pre})).$$

Statistical analysis

Descriptive statistics were carried out using Microsoft Excel 2013 and statistical testing was performed with the software package R (R Foundation for Statistical Computing, version 3.5.2, 2018-12-20). Significance was set at the $p = 0.05$ level. However, all p values are of descriptive nature and are provided in addition to comprehensive SIR data [6].

Wilcoxon signed-rank test of AC-to-lens ΔSIR values was performed to test for its equality with zero (H_0). Multivariate linear regression analysis was performed to correlate ΔSIR with children's age and to adjust for differences in post injection (p.i.) time. A linear as well as an exponential regression model was fitted to the data.

Data availability statement

Data, i.e., anonymized SI measurements, can be obtained at request of any qualified investigator from the corresponding author.

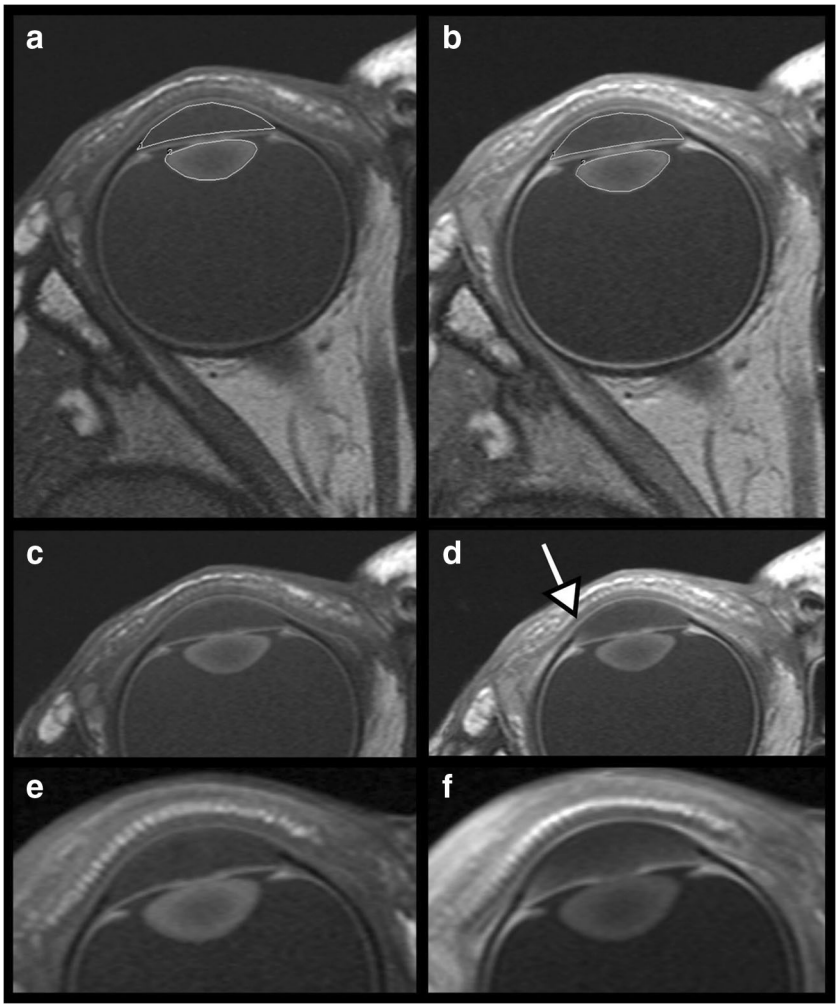

Fig. 1 Example of orbital MRI with applied image analysis and aqueous chamber enhancement. T1-weighted MRI was performed with the children in a state of general anesthesia using bilateral orbital coils prior to (**a**, **c**, **e**) and following following (**b**, **d**, **f**) injection of a standard dose of a macrocyclic gadolinium-based contrast agent (GBCA). **a** and **b** display region of interest (ROI) positioning in the healthy right eye of an 18-month-old boy. The aqueous chamber and lens were delineated on the same slide with the largest diameter for ΔSIR calculation. **c** and **d** provide the same images without ROI placement with the white arrow highlighting GBCA enhancement in the iridocorneal angle on the post injection scan (**d**). **e** and **f** present another case of anterior chamber enhancement following intravenous GBCA injection in a 12-month-old girl

Results

Patient characteristics

Orbital MRI of 200 consecutive treatment naïve patients with unilateral retinoblastoma were included in the study. Average age (± SD) of the patients was 21.9 ± 15.6 months (range 0–91 months). Ninety-eight patients (49.0%) were female and 102 male (51.0%).

One hundred eight (54.0%) left eyes and 92 (46.0%) right eyes were assessed. Mean (range) serum creatinine level was 0.44 (0.19–0.77) mg/dl.

AC-to-lens signal intensity ratios

The median AC-to-lens SIR (interquartile range (IQR)) after GBCA injection was significantly greater than the median SIR (IQR) of the native scan (+ 0.74 (0.70–0.79) vs. + 0.66 (0.63–0.68), paired Wilcoxon test, $p < 0.0001$). Boxplots of SIR values prior to and post GBCA injection are presented in Fig. 2a. Histograms of the two groups revealed a shift of the SIR distribution towards more positive values when comparing SI ratios post injection with SI ratios prior to injection (compare Fig. 2b). Median ΔSIR (IQR) was + 0.08 (0.05–0.12).

Qualitative assessment of the AC revealed a slightly visible SI increase adjacent to the ventral iris with a maximum in the iridocorneal angle in 40 of 200 (20.0%) healthy eyes.

Correlation of signal intensity ratios and children's age

Spearman correlation revealed a strong negative association between children's age and ΔSIR (Spearman's rank correlation coefficient $\varrho = -0.52$, $p < 0.0001$).

To further describe this association, a linear as well as an exponential regression model was fitted to the data.

The linear model (Fig. 3a) followed the equation

$$\Delta SIR = m \times \text{age [months]} + c \mid \text{coefficient estimates:}$$

- intercept $c = 0.16$, $p < 0.0001$
- slope $m = -0.003$, $p < 0.0001$

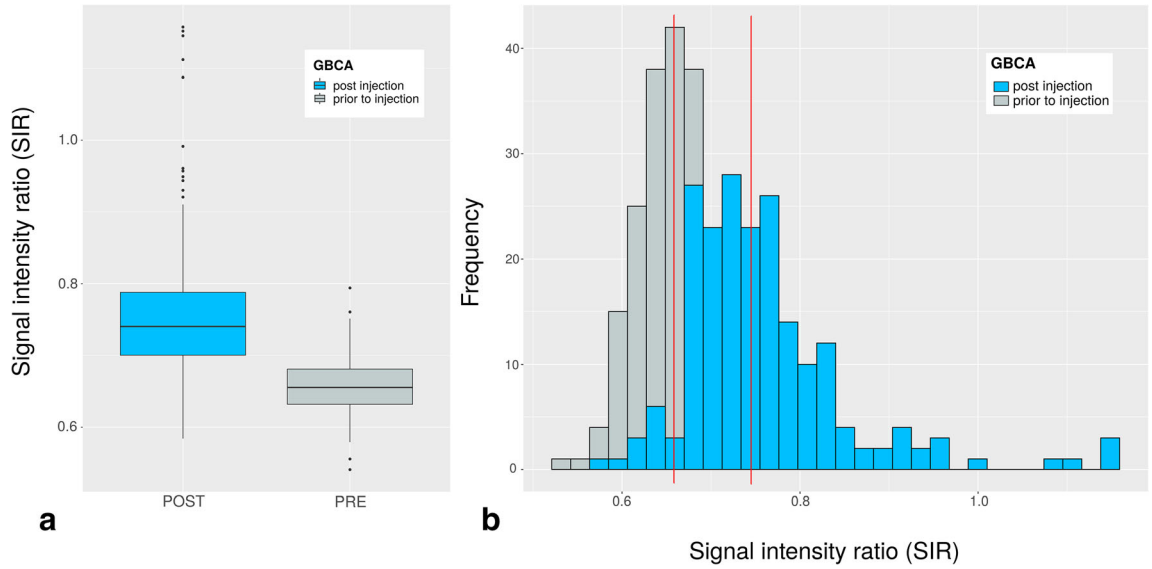

Fig. 2 Comparison of anterior chamber (AC)-to-lens signal intensity ratios (SIRs) prior to and following intravenous injection of a macrocyclic gadolinium-based contrast agent (GBCA). **a** Boxplot of SIRs promptly following GBCA injection (POST) presents higher values compared to the native scan (PRE). Median SIRs of the two groups differed significantly (paired Wilcoxon test, $p < 0.0001$). **b** Accordingly, distribution of SIRs following GBCA injection (blue) was shifted to more positive values compared to native SIRs (gray) in histogram analysis

The exponential model (Fig. 3b) followed the equation

$$\Delta\mathrm{SIR} = \exp.(a + b \times \text{age [months]}) \mid \text{coefficient estimates:}$$

- $a = -1.59$, $p < 0.0001$
- $b = -0.04$, $p < 0.0001$

The exponential fit seems to be superior in describing the data especially for extreme x values, i.e., the youngest and eldest children, indicating an exponential decrease of blood-aqueous barrier permeability and/or exponential increase of outflow capacity with children's age (compare Fig. 4). The residuals are shown in the supplements (Fig. e-2).

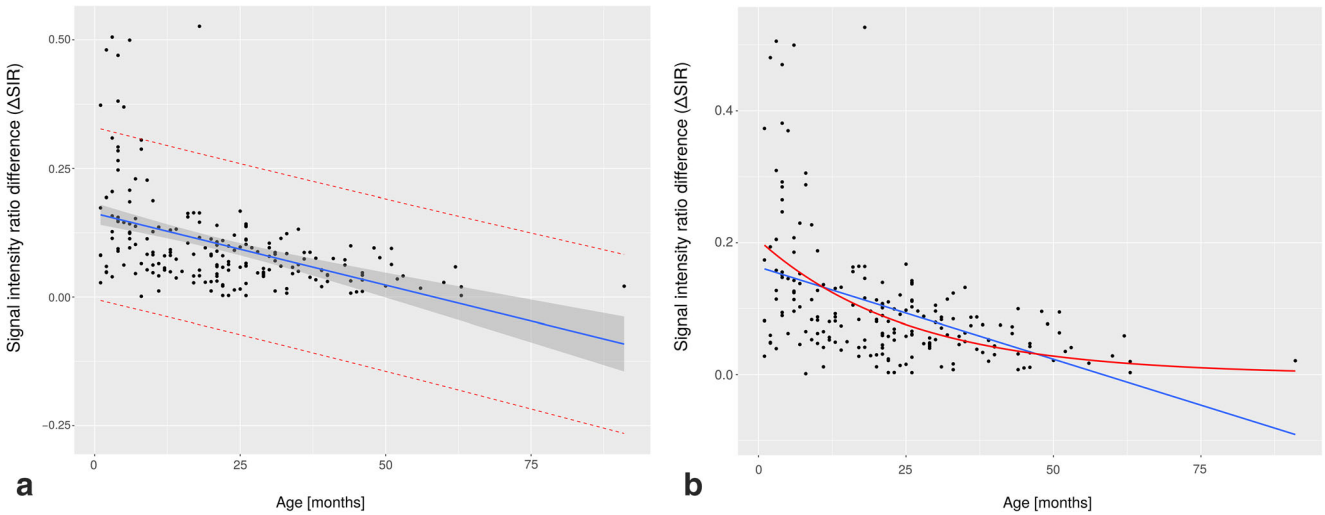

Fig. 3 Scatter plots of signal intensity ratio differences (ΔSIRs) over children's age with presentation of a linear as well as an exponential fitting model. **a** The linear regression model describes the association of the ΔSIR with children's age as follows: $\Delta\mathrm{SIR} = -0.003 \times \text{age} + 0.16$. Gray bands around the fitted line represent the confidence intervals (95% level of confidence) of the regression line; red dotted lines represent the prediction intervals (95% level of probability). Prediction intervals predict the distribution of individual future points, whereas confidence intervals of parameters predict the distribution of estimates of the true population mean that cannot be observed. **b** The exponential regression model (red line) describes the association of the ΔSIR with children's age as follows: $\Delta\mathrm{SIR} = \exp.(-1.59–0.04 \times \text{age})$. Compared to the linear model (blue line), the exponential fit is superior in describing the data especially for extreme x values, i.e., the youngest and eldest children, suggesting an exponential decrease of blood-aqueous barrier permeability and/or exponential increase in outflow capacity with age

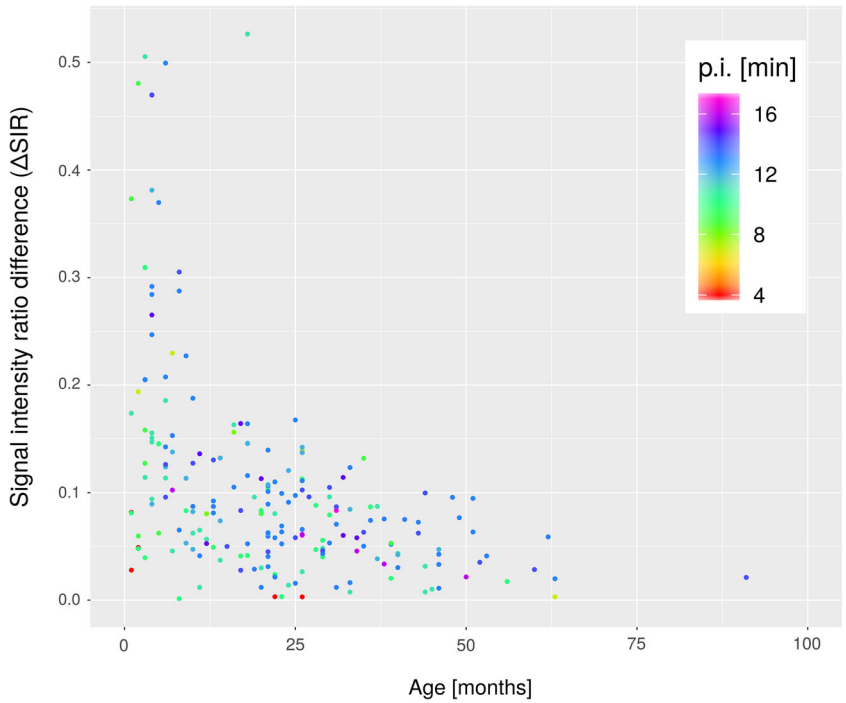

Fig. 4 Scatter plot of anterior chamber-to-lens signal intensity ratio differences (ΔSIRs) over children's age. Different colors of the data points represent different post injection times. ΔSIRs calculated from post contrast scans following immediately after injection of the gadolinium-based contrast agent are low (compare red data points), independent of the children's related age. However, ΔSIRs of long-lasting post injection times did not clearly surpass the others (compare violet data points)

The correlation between ΔSIR and children's age was confirmed in multivariate analysis with adjustment for p.i. time (correlation coefficients: intercept $c = 0.10$, $p = 0.0005$; $m_{age} = -0.003$, $p < 0.0001$; $m_{p.i.\ time} = 0.005$, $p = 0.03$).

Figure 4 illustrates ΔSIRs dependent on children's age and p.i. time, which revealed small ΔSIRs, when the enhanced scan followed GBCA injection very promptly (compare Fig. 4, red data points). However, when excessing a certain injection time, degree of ΔSIR was dominated by children's age rather than p.i. time.

Discussion

In the current study, we demonstrated GBCA infiltration into the aqueous chamber on T1-weighted MRI promptly following GBCA injection that was inversely correlated with the age of children aged 0 to 8 years.

Therewith, the current study generates new knowledge not just with regard to blood-aqueous barrier physiology, which might be exploited for diagnostic and therapeutic applications. Moreover, the study contributes to a growing interdisciplinary field of science which investigates the excretion process of gadolinium tracers—exemplary for all comparable foreign and intrinsic serum constituents—into and through the CNS [1, 7–12].

GBCA passage through the CNS

In 2013, Kanda et al reported on an SI increase of the dentate nucleus due to serial GBCA injections [13], which led to the question of GBCA entry and passage via the CNS as it was supposed to be sealed from the external environment by the blood-brain barrier. Concurrently, Iliff et al proved existence of the glymphatic system (GS), a brain-wide network of CSF microcirculation located in perivascular spaces of penetrating cortical arteries. Mediating CSF-interstitial fluid exchange the GS is said to serve excretory function for elimination of foreign and waste proteins from the CNS [14].

Our study results complement the recently published study of Deike-Hofmann et al who found a SI increase in various cerebral fluid spaces, including the aqueous and vitreous, on delayed T2-weighted GBCA-enhanced MRI 3-h p.i. of a macrocyclic GBCA in neurologically healthy adults [4].

In their study, SI increase was highest in the AC with GBCA drainage from the orbit along the optical nerve into the basal CSF cisterns. With other studies proving brain-wide centripetal distribution of intrathecally injected GBCA tracer from the brain surface far into the deep white matter via the GS [11, 12], a potential afferent pathway for deposition of linear GBCAs was firstly identified. However, exact location and time of GBCA infiltration into the AC remained unclear.

New knowledge regarding blood-aqueous barrier physiology and their implications

Apart from new perceptions regarding GBCA passage into and via the CNS, the current study enabled detailed assessment of anterior eye segment physiology on T1-weighted images due to the ocular coil, which achieved a higher resolution of the eye compared to standard head coils.

Due to the visual finding of a slight SI increase in the AC adjacent to the ventral iris with a maximum in the iridocorneal angle, while no visual SI increase was found in the posterior chamber, we hypothesize an entry into the AC via a known physiological leak of the blood-aqueous barrier at the root of the iris rather than active secretion of the GBCA by the ciliary epithelium into to the posterior chamber.

However, it might be concluded that penetration into the AC can generally be achieved by molecules with similar biochemical and electrophysiological properties as the injected macrocyclic GBCA.

The found negative correlation between the GBCA concentration in the AC and the age of the children aged between 0 and 8 years suggest either a higher blood-aqueous barrier permeability or a lower efflux capacity via the Schlemm's canal in neonates compared to older children.

In the adult eye, it is well known that plasma components easily diffuse out of the fenestrated uveal vessels and permeate the surrounding ciliary body stroma [15], but the mature blood-aqueous barrier is supposed to impede free diffusion into the aqueous, whose composition is quite different from those plasma exudates present in the ciliary body stroma [16].

In contrast, in the developing eye, plasma components such as chloride ions, ascorbic acid, and inulin enter the aqueous either directly by diffusing out of intracameral fenestrated vessels, or, indirectly, by moving from the uveal interstitium at the iridocorneal angle into the anterior chamber [17–19]. Conversely, an increased effectiveness of the blood-aqueous barrier can be observed during development, e.g., in terms of decreased concentrations of proteins and inulin in the ocular fluid [17, 20]. Moreover, it is known that the outflow capacity of the trabecular meshwork of human fetuses increases with age [21, 22].

Clearly, while multiple factors determining aqueous hydrodynamics have yet to be determined, hitherto unknown physiology of aqueous fluid dynamics are of immediate clinical interest: While alterations in efflux performance might be observed in glaucoma, alterations of the blood-aqueous barrier occur in multiple common ocular diseases such as diabetic retinopathy or age-related macular degeneration as well as in neurological diseases such as ischemic brain injury [5, 23, 24]. Furthermore, examination of blood-aqueous barrier function via slit-lamp microscopy or laser flare photometry is used in the diagnosis of anterior uveitis [25, 26]. This implies the diagnostic potential of contrast-enhanced MRI, i.e., qualitative, objective, and non-invasive investigation of the blood-aqueous barrier function combined with morphological assessment beyond the anterior eye segment.

Last but not least, our findings suggest that intravenously administered GBCA not just enters the AC but stands in direct contact with the subretinal space via the vitreous with Deike-Hofmann et al demonstrating extensive and longstanding enhancement of the vitreous following intravenous GBCA injection [4], which might be exploited in terms of intraocular drug delivery.

Implications of presence of GBCA in the AC

Ultimately, potential deposition of GBCAs in the eye might meet the current debate on gadolinium deposition in the brain especially when taking in mind that GBCA trapping was found in the vitreous 24-h post intravenous injection [4]. However, one opinion assumes that chelated and dechelated gadolinium has to be distinguished when debating the presence of gadolinium in the brain [27].

According to this theory, the crossing of the chelated gadolinium, i.e., the intact GBCA, into the CNS via the blood-aqueous barrier and through the CNS via the GS, is supposed to be the natural excretion pathway of the intravenously injected GBCA [4]. Animal experiments showed that macrocyclic GBCAs are nearly totally cleared over time while the less stable linear GBCAs dechelate on the pathway through the brain and potentially remain permanently in areas with an increased metal content [28–30].

From the current study, no conclusions can be drawn regarding the duration of the GBCA in the ocular structures. However, it should be highlighted that the amount of GBCAs penetrating into the eye is presumably extremely small and that the permeability of the blood-aqueous barrier might further decrease in adults. Since approximately half a billion of GBCA injections have already been applied in patients, it seems unlikely that GBCA injections might cause immediate effects on the vision. However, long-term effects after serial injection such as increased risk for cataract development should be investigated.

Strengths and limitations of this study need to be acknowledged. Obvious strength of the study is the large number of assessed eyes with all of them imaged in the same MRI scanner with the same coil and identical sequence parameters.

For limitations, it needs to be pointed out that we did not measure the gadolinium content directly and that T1-weighting is semi-quantitative in nature, that is why the calculated ΔSIRs do not allow drawing conclusions regarding true GBCA concentrations.

Last but not least, serial p.i. scans would have been desirable as the concentration peak of the GBCA in the AC might have exceeded p.i. time and to allow for investigation of orbital GBCA dynamics. However, ΔSIRs of the longest p.i. times did not clearly surpassed the other ΔSIRs, which suggests that AC enhancement might have already reached saturation.

In conclusion, this study revealed an age-dependent GBCA penetration into the anterior chamber of healthy eyes promptly after intravenous injection, which might be exploited for

diagnostic or therapeutic purposes. On the other hand, any potential long-term effects of serial GBCA injection on the vision might be assessed in more detail in future studies.

Acknowledgments We wish to acknowledge the help provided by PD Dr. Holland-Letz, Department of Biostatistics, German Cancer Research Center.

Funding information The authors state that this work has not received any funding.

Compliance with ethical standards

Guarantor The scientific guarantor of this publication is Prof. Alexander Radbruch.

Conflict of interest The authors of this manuscript declare relationships with the following companies:
Alexander Radbruch: Guerbet, Bayer, GE.
Katerina Deike-Hofmann: Guerbet, Bayer, GE.

Statistics and biometry No complex statistical methods were necessary for this paper.

Informed consent Written informed consent was waived by the Institutional Review Board.

Ethical approval Institutional Review Board approval was obtained.

Methodology
• Retrospective
• Observational
• Performed at one institution

References

1. Taoka T, Jost G, Frenzel T, Naganawa S, Pietsch H (2018) Impact of the glymphatic system on the kinetic and distribution of gadodiamide in the rat brain. Invest Radiol 53(9):529–534. https://doi.org/10.1097/RLI.0000000000000473
2. Jost G, Frenzel T, Lohrke J, Lenhard DC, Naganawa S, Pietsch H (2017) Penetration and distribution of gadolinium-based contrast agents into the cerebrospinal fluid in healthy rats: a potential pathway of entry into the brain tissue. Eur Radiol 27(7):2877–2885. https://doi.org/10.1007/s00330-016-4654-2
3. Lohrke J, Frisk A, Frenzel T et al (2017) Histology and gadolinium distribution in the rodent brain after the administration of cumulative high doses of linear and macrocyclic gadolinium-based contrast agents. Invest Radiol 52(6):324–333. https://doi.org/10.1097/RLI.0000000000000344
4. Deike-Hofmann K, Reuter J, Haase R et al (2019) Glymphatic pathway of gadolinium-based contrast agents through the brain: overlooked and misinterpreted. Invest Radiol 54(4):229–237. https://doi.org/10.1097/RLI.0000000000000533
5. Hitomi E, Simpkins AN, Luby M, Latour LL, Leigh RJ, Leigh R (2018) Blood–ocular barrier disruption in acute stroke patients. Neurology. 90(11):e915–e923. https://doi.org/10.1212/WNL.0000000000005123
6. Harrington D, D'Agostino RB, Gatsonis C et al (2019) New guidelines for statistical reporting in the journal. N Engl J Med 381(3):285–286. https://doi.org/10.1056/nejme1906559
7. Taoka T, Naganawa S (2018) Gadolinium-based contrast media, cerebrospinal fluid and the glymphatic system: possible mechanisms for the deposition of gadolinium in the brain. Magn Reson Med Sci 17(2):111–119. https://doi.org/10.2463/mrms.rev.2017-0116
8. Naganawa S, Nakane T, Kawai H, Taoka T (2017) Gd-based contrast enhancement of the perivascular spaces in the basal ganglia. Magn Reson Med Sci 16:61–65. https://doi.org/10.2463/mrms.mp.2016-0039
9. Iliff JJ, Lee H, Yu M et al (2013) Brain-wide pathway for waste clearance captured by contrast-enhanced MRI. J Clin Invest 123(3):1299–1209. https://doi.org/10.1172/JCI67677
10. Kress BT, Iliff JJ, Xia M et al (2014) Impairment of paravascular clearance pathways in the aging brain. Ann Neurol 76(6):845–861. https://doi.org/10.1002/ana.24271
11. Ringstad G, Valnes LM, Dale AM et al (2018) Brain-wide glymphatic enhancement and clearance in humans assessed with MRI. JCI Insights 3(13):1–17. https://doi.org/10.1172/jci.insight.121537
12. Ringstad G, Vatnehol SAS, Eide PK (2017) Glymphatic MRI in idiopathic normal pressure hydrocephalus. Brain. 140(10):2691–2705. https://doi.org/10.1093/brain/awx191
13. Kanda T, Ishii K, Kawaguchi H, Kitajima K, Takenaka D (2013) High signal intensity in the dentate nucleus and globus pallidus on unenhanced T1-weighted MR images: relationship with increasing cumulative dose of a gadolinium-based contrast material. Radiology. 270(3):834–841. https://doi.org/10.1148/radiol.13131669
14. Iliff JJ, Wang M, Liao Y et al (2012) A paravascular pathway facilitates CSF flow through the brain parenchyma and the clearance of interstitial solutes, including amyloid b. Sci Transl Med 4(147):ra111. https://doi.org/10.1126/scitranslmed.3003748
15. Bill A (1968) Capillary permeability to and extravascular dynamics of myoglobin, albumin and gammaglobulin in the uvea. Acta Physiol Scand 73(1–2):204–219. https://doi.org/10.1111/j.1748-1716.1968.tb04097.x
16. Raviola G (1977) The structural basis of the blood-ocular barriers. Exp Eye Res 25(1):27–63. https://doi.org/10.1016/S0014-4835(77)80009-2
17. Kinsey VE, Williamson MB (1949) Investigation of the blood-aqueous barrier in the newborn. II To inulin. Am J Ophthalmol 32(4):509–512. https://doi.org/10.1016/0002-9394(49)90875-2
18. Kinsey E, Blanche J, Terry TL (1945) Development of secretory function of ciliary body in the rabbit eye evaluated from ascorbic acid concentrations and changes in volume. J Gen Physiol 34(5):415–417. https://doi.org/10.1001/archopht.1945.00890190419013
19. Kinsey VE, Jackson B (1949) Investigation of the blood-aqueous barrier in the newborn. I. To ascorbic acid. Am J Ophthalmol 32(3):374–378. https://doi.org/10.1016/0002-9394(49)91930-3
20. Bembridge BA, Pirie A (2015) Biochemical and histological changes in developing rabbit eyes. Br J Ophthalmol 35(12):784–789. https://doi.org/10.1136/bjo.35.12.784
21. Kupfer C, Ross K (1971) The development of outflow facility in human eyes. Invest Ophthalmol 10(7):513–517 https://iovs.arvojournals.org/
22. Pandolfi M, Åstedt B (1971) Outflow resistance in the foetal eye. Acta Ophthalmol (Copenh) 49(2):344–350. https://doi.org/10.1111/j.1755-3768.1971.tb00959.x
23. Oshika T, Kato S, Funatsu H (1989) Quantitative assessment of aqueous flare intensity in diabetes. Graefes Arch Clin Exp Ophthalmol 227(6):518–520. https://doi.org/10.1007/BF02169443

24. Kubota T, Küchle M, Nguyen NX (1994) Aqueous flare in eyes with age-related macular degeneration. Jpn J Ophthalmol 38(1):67–70
25. Chen M-S, Hou P-K, Tai T-Y, Lin BJ (2008) Blood-ocular barriers. Tzu Chi Med J 20(1):25–34. https://doi.org/10.1016/S1016-3190(08)60004-X
26. Sawa M (2017) Laser flare-cell photometer: principle and significance in clinical and basic ophthalmology. Jpn J Ophthalmol 61(1):21–42. https://doi.org/10.1007/s10384-016-0488-3
27. Radbruch A, Roberts DR, Clement O, Rovira A, Quattrocchi CC (2017) Chelated or dechelated gadolinium deposition. Lancet Neurol 16(12):955. https://doi.org/10.1016/S1474-4422(17)30365-4
28. Radbruch A, Richter H, Fingerhut S et al (2019) Gadolinium deposition in the brain in a large animal model. Invest Radiol 54(9):531–536. https://doi.org/10.1097/RLI.0000000000000575
29. Robert P, Fingerhut S, Factor C et al (2018) One-year retention of gadolinium in the brain: comparison of gadodiamide and gadoterate meglumine in a rodent model. Radiology. 288(2):424–433. https://doi.org/10.1148/radiol.2018172746
30. Jost G, Frenzel T, Boyken J, Lohrke J, Nischwitz V, Pietsch H (2018) Long-term excretion of gadolinium-based contrast agents: linear versus macrocyclic agents in an experimental rat model. Radiology. 290(2):340–348. https://doi.org/10.1148/radiol.2018180135